Altered focal adhesion regulation correlates with cardiomyopathy in mice expressing constitutively active rac1

Mark A. Sussman,[1] Sara Welch,[1] Angela Walker,[1] Raisa Klevitsky,[1] Timothy E. Hewett,[1] Robert L. Price,[2] Erik Schaefer,[3] and Karen Yager[4]

[1]The Children's Hospital and Research Foundation, Division of Molecular Cardiovascular Biology, Cincinnati, Ohio 45229, USA
[2]University of South Carolina, Department of Developmental Biology and Anatomy, University of South Carolina School of Medicine, Columbia, South Carolina 29208, USA
[3]QCB Biosource International, 3 Avenue D, Hopkinton, Massachusetts 01748, USA
[4]The Children's Hospital and Research Foundation, Transgenic Core Facility, Cincinnati, Ohio 45229, USA

Address correspondence to:Mark A. Sussman, The Children's Hospital and Research Foundation, Division of Molecular Cardiovascular Biology, Room 3033, 3333 Burnet Avenue, Cincinnati, Ohio 45229, USA. Phone: (513) 636-7145; Fax: (513) 636-8966; E-mail: sussman@heart.chmcc.org.

Received for publication September 21, 1999, and accepted in revised form February 14, 2000.

The ras family of small GTP-binding proteins exerts powerful effects upon cell structure and function. One member of this family, rac, induces actin cytoskeletal reorganization in nonmuscle cells and hypertrophic changes in cultured cardiomyocytes. To examine the effect of rac1 activation upon cardiac structure and function, transgenic mice were created that express constitutively activated rac1 specifically in the myocardium. Transgenic rac1 protein was expressed at levels comparable to endogenous rac levels, with activation of the rac1 signaling pathway resulting in two distinct cardiomyopathic phenotypes: a lethal dilated phenotype associated with neonatal activation of the transgene and a transient cardiac hypertrophy seen among juvenile mice that resolved with age. Neither phenotype showed myofibril disarray and hypertrophic hearts were hypercontractilein working heart analyses. The rac1 target p21-activated kinase translocated from a cytosolic to a cytoskeletal distribution, suggesting that rac1 activation was inducing focal adhesion reorganization. Corroborating results showed altered localizations of src in dilated cardiomyopathy and paxillin in both cardiomyopathic phenotypes. This study, the first examination of rac1-mediated cardiac effects in vivo, demonstrates that dilation and hypertrophy can share a common molecular origin and presents evidence that both timing and concurrent signaling from multiple pathways can influence cardiac remodeling.

J. Clin. Invest. **105**:875–886 (2000).

Introduction

Small GTP-binding proteins, including ras, rho, and rac, participate in diverse cellular functions such as locomotion, cytokinesis, and cytoskeletal remodeling in nonmuscle cells (1–4). Although these cellular functions seem superficially irrelevant for normal myocardial function, activation of such programs in differentiated cardiomyocytes has significant effects. Specifically, changes resulting from activation of rac- or rho-mediated cellular remodeling in cardiomyocytes (5, 6) suggest that myocardial architecture responds to the same signals that induce cytoskeletal reorganization in nonmuscle cells.

Reports on the cardiac-based effects of ras, rho, and rac indicate that their primary action is to modulate hypertrophic responses (7, 8). Ras-mediated cardiac hypertrophy has been demonstrated both in vitro (9) and in vivo (10), whereas a transgenic (tg) mouse cardiomyopathy model created by rhoA overexpression characterized the resultant disease as a conduction abnormality leading to ventricular failure (11). Severely affected mice exhibited symptoms consistent with loss of systolic function and dilated cardiomyopathy. This finding for the rhoA effect in vivo was unanticipated, because several in vitro studies had previously implicated rhoA in development of hypertrophic responses (6, 12, 13).

In comparison, studies of rac1-mediated effects have only described effects on cultured cardiomyocytes (5, 6). Hypertrophic remodeling of cultured cardiomyocytes resulted from introduction of constitutively activated V12rac1 (5). This study also showed a requirement for rac activation in phenylephrine-induced cardiomyocyte hypertrophy, which was inhibited by expression of a dominant-negative N17rac1 construct. These studies have provided significant clues into the biological activity of rac and rho in the context of the myocardium. However, the functional effect upon cytoskeletal organization, for which these regulatory molecules initially achieved notoriety, has remained unexplored.

Rac is able to exert control over hypertrophic responses because, like ras, rac is positioned at the top of a cellular cascade mediating multiple signaling effects

involving various downstream target molecules. Although they are not kinases themselves, the ras family of small GTP-binding proteins regulates signaling pathways that activate mediators of phosphorylation. Rac and rho activation initiate a cascade of signal amplification involving downstream target proteins such as mitogen-activated protein kinase (MAPK) or jun NH_2-terminal kinase (JNK) family members (14, 15), p21-activated kinase (PAK; 16, 17), and focal adhesion kinase (FAK; 18). Activation of these kinases presumably alters cardiomyocyte protein phosphorylation, with MAPK or JNK signaling resulting in hypertrophy (19). However, the effects of other rac- and rho-activated kinases upon cardiac structure and function remain largely unexplored. The association of rac- and rho-mediated pathways with remodeling of cell shape and actin cytoskeletal structure (1–4) suggests these regulatory proteins are likely to be involved with cardiac adaptation, remodeling, and the pathogenesis of cardiomyopathies characterized by cellular enlargement and/or reorganization of adhesion contacts.

Widespread cytoskeletal remodeling and adhesion reorganization after the activation of rac1 in fibroblasts seems unlikely in mature cardiomyocytes of the functioning myocardium, where contractile function depends upon a highly organized cytoskeleton and stable cellular adhesion. However, loss of cellular adhesion would be consistent with the progression of dilated cardiomyopathy and concomitant deterioration of systolic performance. To examine this possibility, tg mice were created to express constitutively activated rac1 specifically in the myocardium. Analysis of these rac1-expressing tg (racET) mice revealed phenotypes consistent with previous in vitro functional characterizations of rac. First, racET mice develop hypertrophic changes within weeks after birth, indicating that rac1 mediates cardiac hypertrophy in vivo. Second, signaling pathways controlling focal adhesions are deregulated in racET mice, and focal adhesion structures appear altered. These effects are consistent with the hypothesis that rac1 controls the actin cytoskeleton. Third, elevation of rac1 activity in neonatal racET mice results in lethal dilated cardiomyopathy associated with a marked alteration of cellular adhesion structures. Severe dilation present in young racETs, together with the lack of overt myofibril degeneration as assessed by confocal and electron microscopy, suggests that a loss of cytoskeletal-based cardiomyocyte adhesion can result in dilated cardiomyopathy and heart failure. These results extend previous in vitro characterizations of rac1 to an in vivo environment and provide the first description of an experimentally induced dilated cardiomyopathy associated with deregulation of cardiomyocyte focal adhesions.

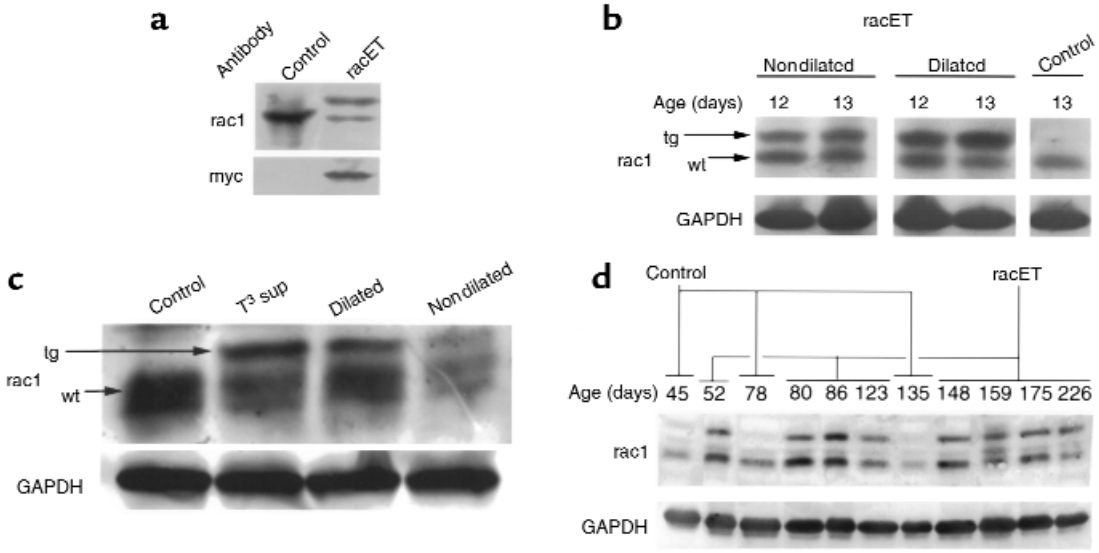

Figure 1

Expression level of rac1 and V12rac1 transgene in heart lysates by immunoblot. Control and racET heart lysates were separated by SDS-PAGE, blotted, and the region corresponding to the molecular mass of rac1 (21 kDa) was excised for antibody labeling. GAPDH signal shows loading of samples between lanes. (**a**) Ntg (control) or racET samples were labeled for rac1 (rac) or myc (myc) to reveal presence of myc-tagged transgene. The control shows a single band of rac1, whereas the racET shows a doublet. The lower band of the doublet corresponds to endogenous rac1, and the upper band is myc-tagged transgene. An identically prepared blot shows myc-tagged protein appearing as a single band in the racET lysate. (**b**) Comparison of transgene expression between racET and control shows increased rac1 transgene expression in dilated samples. Arrows indicate position of transgenic (tg) or endogenous (wt) rac1. (**c**) Comparison of transgene expression between lysates from ntg (control), T^3 supplemented (T^3 sup), and dilated or nondilated racET hearts. T^3 supplementation elevated expression relative to control, resembling the level in dilated racET mice, whereas the nondilated sample shows less protein. (**d**) Rac1 expression in ntg (control) or racET hearts ranging in age from 45 to 226 days after birth. Variable but persistent transgene expression is evident in racET lysates, whereas only endogenous rac1 is observed in control samples.

Methods

Construction of the α-myosin heavy chain (MHC)-rac1 transgene. The α-5.5 wild-type promoter has been described previously (20) and tested in vivo (21). Full-length rac1 cDNA encoding constitutively activated protein (22; provided by A. Hall, MRC Laboratory for Molecular Cell Biology, University College London, London, United Kingdom) was inserted downstream from the α-MHC promoter in a unique SalI restriction site of the plasmid (clone 26; provided by J. Robbins, The Children's Hospital Research Foundation, Cincinnati, Ohio, USA).

Creation and breeding of racET mice. DNA constructs were prepared for injection as described previously (23). Samples of genomic DNA were screened by PCR for presence of the transgene using primers from the promoter region (5′-GGCAGGGAAGTGGTGGTGTAGGAA-3′) and the transgene reverse primer (5′-ATCATCCCTAAGATCAAGTTTAGTTCCCAC-3′) producing a 350-bp-long product. Ten potential founders were subsequently screened by genomic Southern blot analysis. Five different founder lines (57, 63, 68, 80, and 9.1) with the highest transgene copy signal were selected. Each line was bred to homozygosity and offspring were screened by immunoblot analysis for rac1 protein expression. The line with the highest expression (line 63) was selected for study. Other lines showed similar cardiac effects, as did breeding between line 63 and lines with lower expression levels (data not shown).

Phenotype tracking and database analysis. Data gathered on racET mice was analyzed using Progeny (Progeny Software LLC, South Bend, Indiana, USA), which combines relational database tools with a pedigree drawing function.

Gross heart preparation and photography. After CO_2 asphyxiation, hearts were immediately removed and prepared for fixation using one of the following: [a] blood was removed by flushing with relaxing buffer (5% dextrose, 25 mM KCl in PBS) administered by gravity flow through a needle inserted into the apex of the heart; [b] the heart was placed in relaxing buffer and blood was expelled from the chambers by gently applying pressure to the heart walls; or [c] the heart was placed directly into fixative. Hearts were fixed in Histoprep formalin (No. HC-200; Fisher Scientific Co., Pittsburgh, Pennsylvania, USA) and then bisected. Bisected hearts were photographed and converted into digitized images.

Thyroid hormone manipulations. Mice were supplemented with thyroid hormone (3,3′,5-triiodo-L-thyronine [T^3]) (T-6397; Sigma Chemical Co., St. Louis, Missouri, USA) at 3 days after birth for 5 days. Dosage (100 μg/100 ml) in drinking water was determined empirically to lack discernable effects upon nontransgenic (ntg) controls. T^3 was prepared as described previously (24). Hypothyroidism was induced by diet supplementation with 5-propyl-2-thiouracil (PTU) in the food, which has been shown to inhibit α-MHC promoter–driven transgene expression (25).

Determination of mRNA expression levels. Total heart mRNA was subjected to Northern blot analysis using

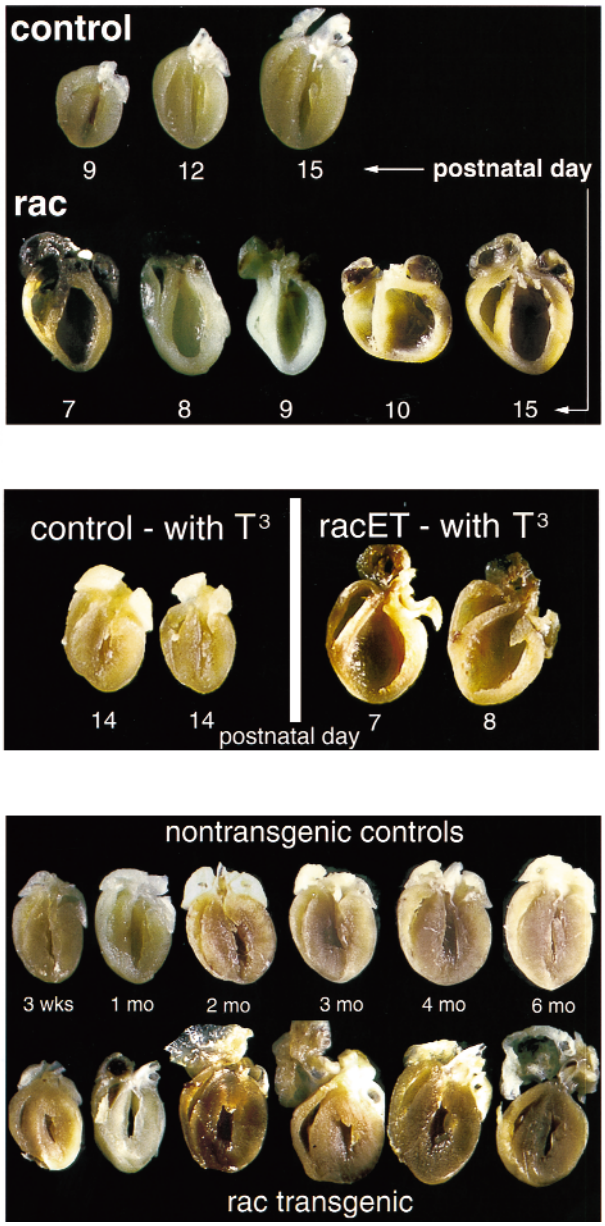

Figure 2
Gross morphology of dilated and hypertrophic racET hearts. (Top) Bisected racET hearts ranging from 7 to 15 days of age (bottom row) compared with typical ntg control hearts shown at 9, 12, and 15 days for comparison (top row). Ntg control hearts show a progressive increase in heart size consistent with rapid postnatal growth in this period. In comparison, racET hearts are enlarged with severely dilated chambers and thin ventricular walls. Atria are also increased in size relative to ntg controls, although to a lesser degree than ventricles. (Middle) Postnatal thyroid hormone supplementation correlates with development of racET cardiomyopathy. Hearts from ntg control mice developed normally without apparent morphologic effects from supplementation (left, shown at 2 weeks of age). In contrast, hearts from supplemented racET mice all developed lethal dilated cardiomyopathy within 1.5 weeks after birth. (Bottom) Bisected hearts ranging from 3 weeks to 6 months of age for ntg controls (top row) and racET mice (bottom row). Concentric hypertrophy is evident in the 3-week-old racET ventricles, but hypertrophic characteristics diminish as the mice age. In contrast, atria in racET mice show severe enlargement by 2 months after birth and continued deterioration as the mice age.

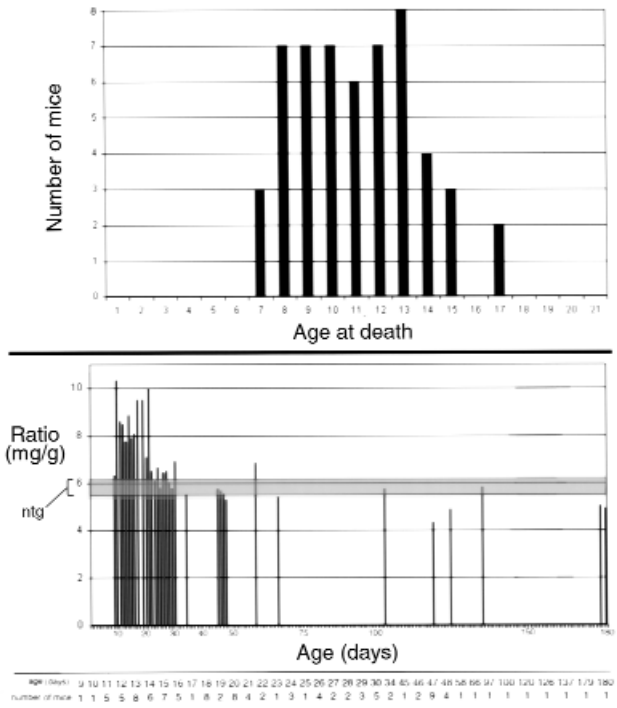

Figure 3
Analysis of spontaneous mortality and hypertrophic heart/body weight ratio normalization in the racET population. (Top) Plot of age at death (x-axis) versus number of mice that died (y-axis) for 54 racET mice dead within 3 weeks after birth. Postmortem examination of this population revealed every mouse had dilated cardiomyopathy (see Figure 2). Mortality was evident as early as 7 days after birth, with a high level of mortality present throughout postnatal days 8–13. (Bottom) Plot of age (x-axis) versus heart/body weight ratio (mg/g) for 98 racET mice found to have hypertrophic hearts at time of sacrifice. Range of average ratios for control mice are indicated within the shaded area (ntg). Ntg control heart/body weight ratios are 6.06 ± 0.6 mg/g under 1 month of age and 5.5 ± 0.6mg/g for mice over 1 month of age. Ratios for young racET mice are higher within the first month after birth (7.22 ± 2.15; $n = 71$) compared with mice over 1 month of age (5.86 ± 0.86; $n = 20$). This ratio versus ntg controls shifted from statistically significant in mice under 1 month of age ($P = 0.015$) to insignificance in older mice ($P = 0.154$) indicating a normalization of heart/body weight ratio as racET mice age. The number of racET mice averaged for each time point is shown at the bottom of the graph.

antisense oligonucleotide probes (23). Significance determinations were calculated by Student's *t*-test analysis relative to the signal measured for myosin light chain (MLC) 2V . Variations in sample loading were normalized relative to GAPDH signal. Samples were collected from hearts of racET mice 14–25 days old, that had been classified as hypertrophic based on characteristics of elevated heart/body weight ratio and a lack of ventricular chamber dilation. Age-matched ntg mice were used as control samples.

Microscopic analyses. For fluorescent antibody staining, sections were prepared from hearts fixed in 4% paraformaldehyde/PBS overnight at 4°C. The next day, hearts were subjected to a progressive sucrose gradient from 10%, 20%, and 30% at 4°C for 1 hour at each step, embedded in Tissue-Tek (Fisher Scientific Co.), frozen in melting isopentane floated above liquid nitrogen, and frozen blocks were stored at –80°C. Sections 7 μm thick were mounted on Superfrost slides (Fisher Scientific Co.), allowed to dry, and then stored at 4°C until use within 1 week. For labeling, primary antibodies were applied to the sections and left overnight. The next day, sections were washed, secondary antibodies were applied to the sections for 1 hour, washed again, and then mounted in Vectashield (Vector Laboratories, Burlingame, California, USA). Primary antibodies applied to sections were directed against α-actinin (Sigma Chemical Co.), PAK (Santa Cruz Biotechnology Inc., Santa Cruz, California, USA), myc-tag (Upstate Biotechnology Inc., Lake Placid, New York, USA), rac1 (Upstate Biotechnology Inc.), paxillin (Transduction Laboratories, Lexington, Kentucky, USA), and phosphothreonine (Sigma Chemical Co.). In addition, antibodies directed against phosphorylated sites on signaling proteins included src^{418}, src^{529}, FAK^{843}, and paxillin[31] (all from Biosource International, Camarillo, California, USA). Primary antibodies were detected by fluorescent secondary goat anti-mouse IgG (Cy 5; Jackson ImmunoResearch Laboratories, West Grove, Pennsylvania, USA) and goat anti-rabbit IgG (FITC; Sigma Chemical Co.). Cell-permeable stains included ToPro.3 to label nuclei (Molecular Probes Inc., Eugene, Oregon, USA) and Texas red–tagged phalloidin to label actin filaments (Molecular Probes Inc.). Single cardiomyocytes were prepared for fluorescence labeling and viewed by confocal microscopy as described previously (26). Confocal microscopy was performed as described previously (23).

Biochemical analyses. Freshly isolated hearts were minced, washed in extraction buffer (20 mM sodium phosphate, pH 7.0, 150 mM sodium chloride, 2 mM magnesium chloride, 0.1% Nonidet P-40, 10% glycerol, 10 nM okadaic acid, 100 μM phenylasine oxide, 10 μg/mL each of pepstatin, leupeptin, aprotinin, TLCK, and TPCK, 10 mM sodium fluoride, 10 mM sodium pyrophosphate, 1 mM DTT, 0.1 mM sodium orthovanadate) and then homogenized in extraction buffer containing 0.1% Triton X-100. Homogenates were spun, supernatants were collected, and protein was precipitated. The pellet was resuspended in loading buffer, boiled, and then loaded onto gels for separation by electrophoresis. Proteins were transferred from the gel to nitrocellulose, proteins were visualized by staining with Ponceau-S (Sigma Chemical Co.), and the region of the blot corresponding to the protein of interest was excised from the blot. After blocking, the blot was washed, primary antibody was added, and then incubated overnight at 4°C. The next morning the blot was washed, and bound antibody was detected using enhanced chemifluorescence (Vistra ECF kit; Amersham Life Sciences Inc., Arlington Heights, Illinois, USA). For weak signals, additional sensitivity was added using alkaline phosphatase anti-alkaline phosphatase (APAAP) reagent (Dako A/S, Glostrup, Denmark).

Table 1
Hypertrophic racET hearts are hypercontractile in isolated heart preparations (means ± SEM)[A]

Measured parameter	ntg control	racET	% change
Working heart	(*n* = 2)	(*n* = 2)	
heart rate (beats/min)	380 ± 1	379 ± 1	Paced
+dP/*dt* (mm Hg/ms)	5,214 ± 224	7,070 ± 290	+36%[B]
–dP/*dt* (mm Hg/ms)	4,342 ± 110	4,453 ± 145	+3%
Langendorff heart	(*n* = 2, 20)	(*n* = 2, 20)	
heart rate (beats/min)	379 ± 1	378 ± 2	Paced
+dP/*dt* (mm Hg/ms)	2,324 ± 21	3,398 ± 59	+46%[B]
–dP/*dt* (mm Hg/ms)	1,643 ± 50	2,658 ± 40	+62%[B]

[A]Working heart preparations were performed using 6-week-old mice as previously described (52). [B]$P \leq 0.001$, transgene versus control, unpaired Student's *t*-test.

Labeled blots were analyzed using a Storm 860 and Imagequant software (both from Molecular Dynamics, Sunnyvale, California, USA).

For immunoprecipitation experiments, lysates were prepared by freezing excised hearts in liquid nitrogen and crushing the heart to powder. Samples were placed in 300 μL of ice-cold lysis buffer (27), briefly sonicated, centrifuged, and the supernatant was harvested. Protein concentration was determined by Bradford assay (Bio-Rad Laboratories Inc., Hercules, California, USA), and 1 mg of total protein was suspended in a final volume of 0.5 mL lysis buffer. Immunoprecipitating antibodies directed against src (Upstate Biotechnology Inc.) or paxillin (Transduction Laboratories) were added and the mixture was placed on a rotator at 4°C for 1 hour. Protein Plus A/G agarose (Santa Cruz Biotechnology Inc.) was added, and the mixture was incubated at 4°C overnight. The next morning, agarose slurry was collected, supernatant was discarded, the agarose pellet was washed 3 times, and sample buffer was placed upon the agarose pellet after the final wash. Samples were boiled, loaded onto SDS gels, separated by electrophoresis, transferred to nitrocellulose, and the remainder of the procedure was performed as described for immunoblot analysis.

Adenoviral infections and analyses of cultured cardiomyocytes. Adenovirus constructs and neonatal rat cardiomyocyte cultures were prepared as described previously (28). Recombinant virus was created using the V12rac1 cDNA fragment carried by racET mice. Cardiomyocyte cultures were infected at a multiplicity of infection of approximately 5 plaque-forming units per cell. After infection for 2 hours, infection medium was aspirated and replaced with maintenance media. Cells were used for experimental analyses the next day, approximately 24 hours after infection. Lysates were prepared from culture dishes as described for preparation of heart samples (see "Biochemical analyses"). Microscopy was performed using cardiomyocytes cultured on plastic chamber slides coated with laminin. For inhibition of tyrosine kinase, cultures were treated with 200 μM genistein (Sigma Chemical Co.) that was added to the replacement medium after infection of the culture with adenovirus.

Results

Low expression of rac1 transgene is consistent with endogenous rac1 protein level. Antibody to rac1 labeled a band with a molecular weight of 21,000 in both lysates, demonstrating that rac1 is normally present in the heart (Figure 1a). In comparison, heart lysate from racET mice showed an additional immunoreactive band with slightly higher M_r derived from expression of the transgene carrying the myc tag. Endogenous rac1 protein levels were decreased 21% ± 12% in racETs (n = 15) relative to ntg controls (n = 7), which is a significant change (P = 0.014). Ntg and racET mice heart lysates labeled with antibody to myc produced a single band in the racET sample with mobility identical to the upper band from the rac1 antibody–labeled racET sample, indicating that this protein was the myc-tagged rac1 transgene. These results indicate that the rac1 transgene was produced in hearts of racET mice, and, more importantly, constitutively activated rac1 transgene protein accumulation was comparable to endogenous levels.

Morphologic changes in hearts of racET mice show two different phenotypic groups, and mortality correlates with dilated cardiomyopathy. A severe dilated phenotype was evident in gross morphology of bisected hearts from racET mice that died within 2 weeks after birth (Figure 2, top). Hearts showed marked enlargement of both ventricles and atria as well as thinning of ventricular walls and the

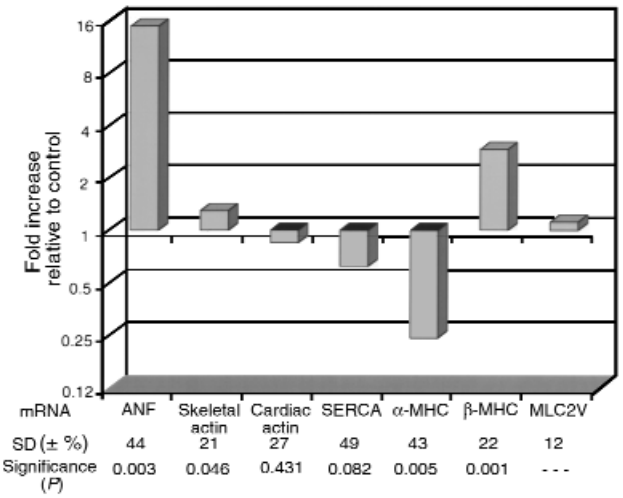

Figure 4
Comparison of mRNA expression levels in hearts of racET mice. Analyses of cardiac gene expression for genes that may be involved in hypertrophic/failure responses. Results are shown as fold increase for racET mice mRNA relative to ntg levels. Equivalent expression between controls and racET mice is presented as 1 (baseline) with values above and below 1 representing increased and decreased expression, respectively. Values were determined from average expression of five individual racET samples. Standard deviations (SD) are percent variation of fold increase. Significance was calculated relative to MLC-2V. Error bars represent standard error of the mean. Signals were normalized for variations in loading with respect to GAPDH. ANF, atrial natriuretic factor; SERCA, sarco/endoplasmic reticulum Ca^{2+}-ATPase.

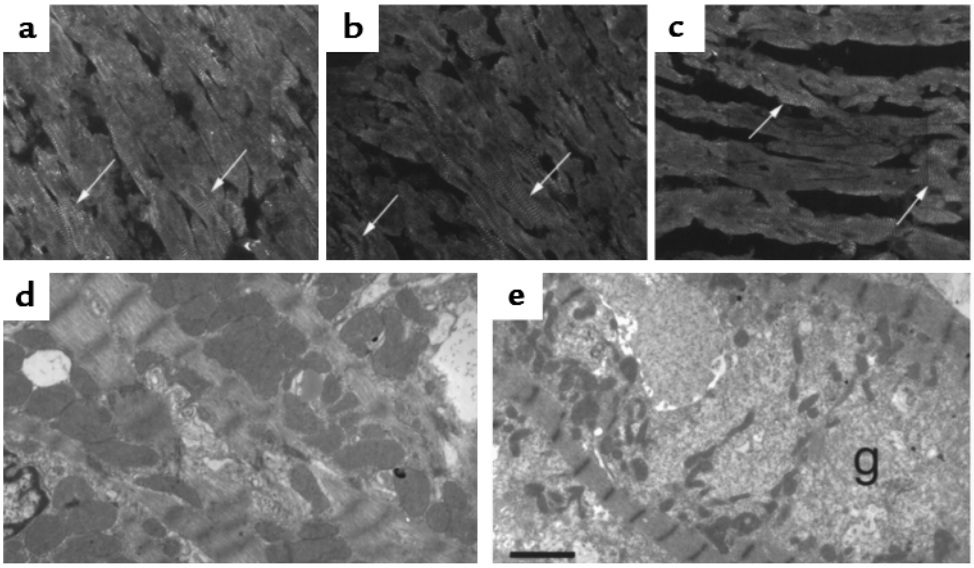

Figure 5
Myofibril organization in racET hearts is not disrupted. Confocal (**a**–**c**) and electron microscopy (**d**–**e**) showing myofibril organization in control ntg (**a**, **d**) or racET (**b**, **c**, **e**) heart sections. Organized Z-discs labeled with α-actinin antibody showed typical striated patterns in control (**a**), dilated racET (**b**), and hypertrophic racET (**c**) sections. Electron microscopy shows normal cardiomyocyte interior (**d**) in comparison with racET cardiomyocyte (**e**) containing granular material (**g**) occasionally observed near the cell center. Electron microscopy samples were prepared and viewed as described previously (51). Bar: (**a**–**c**) 30 μm; (**d**) 7.7 μm; and (**e**) 3.2 μm.

septum. Cardiac morphology from dilated racET mice often showed aberrant "teardrop" (days 8 and 9) or "pumpkin" (day 10) shapes, although enlarged hearts with typical dilated changes were also present (days 7 and 15). This phenotype was associated with high postnatal mortality as shown by population analysis (Figure 3, top). Data gathered on a population of 54 racET mice that died spontaneously within 3 weeks after birth showed peak mortality occurring between 1 and 2 weeks after birth with all the hearts appearing dilated. Premature mortality was limited to 3 weeks after birth because, after this time period, racET mice survival is comparable to normal mice.

Postnatal mortality (Figure 3) could be hypothetically explained by greater rac1 transgene activity in racET mice succumbing to dilated cardiomyopathy, an idea that was supported by 3 lines of evidence enumerated in this paragraph. First, immunoblot analysis of transgene rac1 expression in dilated hearts of racET mice (n = 8; Figure 1b), which was increased an average of 1.9- ± 1.0-fold relative to racET hearts not showing dilated remodeling (n = 7) at this age. However, this difference was not statistically different (P = 0.24) because of the wide standard deviation of expression in the dilated racET mouse population. Second, nondilated hearts from young racET mice (7–10 days) average a 49% decrease in rac1 protein expression relative to ntg controls, never showing high level transgene expression as evident in dilated racET mice (nondilated; Figure 1c). Third, increased postnatal expression of the rac1 transgene was induced using thyroid hormone responsiveness of the α-MHC promoter in the racET mouse. Temporary elevation of postnatal T^3 levels was accomplished by supplementation with 100 μg/mL T^3 in the water for 5 days (3–7 days after birth). This time course for supplementation, designed by empirical testing, was chosen to minimize adverse effects for ntg control mice while still providing high-level T^3 stimulation. Immunoblot results showed increased transgene expression in T^3 supplemented racET mice (Figure 1c, T^3 sup, tg arrow) relative to a ntg control sample (Figure 1c, control). Transgene expression in the T^3-supplemented sample was increased 1.8-fold (n = 5) relative to levels in dilated racET mice (n = 7; Figure 1c, dilated), a statistically significant increase (P = 0.0002). Comparably aged, nondilated racET mice often showed lower rac1 expression (Figure 1c, nondilated), indicating association between transgene expression level and cardiac phenotype. T^3 supplementation had no overt effect upon ntg controls, but caused a marked shift in phenotype toward severe dilated cardiomyopathy in racET mice (Figure 2, middle). T^3-supplemented ntg controls showed no mortality and normal heart/body weight (mg/g) ratios (6.7 ± 0.6, n = 19) comparable to untreated ntg mice (6.1 ± 0.7, n = 32). In contrast, T^3-supplemented racET mice had elevated heart/body weight ratios (16.3 ± 4.5, n = 35) and significant dilation of ventricular chambers, ending in postnatal mortality by 2 weeks of age. These results indicate that dilated cardiomyopathy in neonatal racET mice can be induced by increasing rac1 transgene expression by T^3 stimulation in early postnatal development. Conversely, if racET dilated cardiomyopathy depended upon high level postnatal transgene expression, then inhibition of postnatal rac1 transgene expression should prevent development of dilation. This hypothesis was tested by manipulation of postnatal thyroid hormone level with PTU to induce

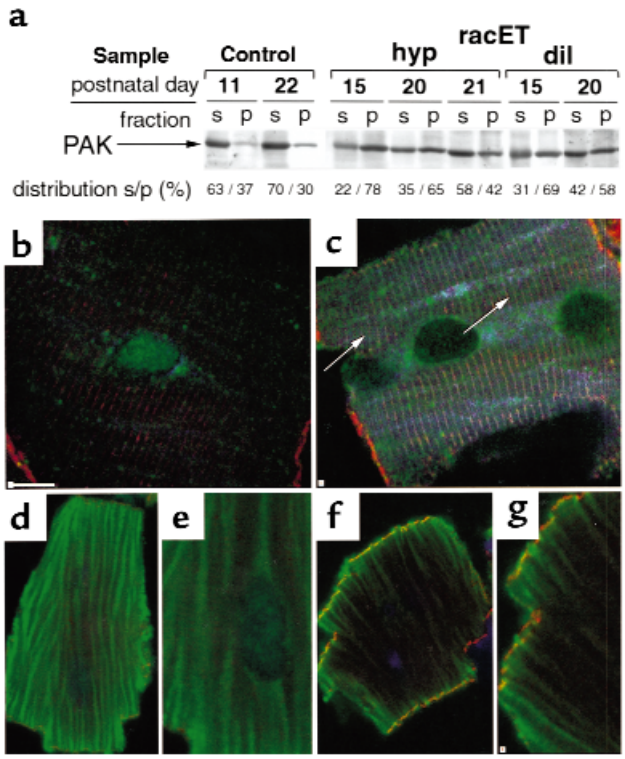

Figure 6
PAK activation and altered phosphothreonine distribution in racET hearts. Immunoblot (**a**) and isolated cardiomyocytes (**b** and **c**) labeled with anti-PAK (**a**–**c**) or antiphosphothreonine (**d**–**g**) antibody. (**a**) Immunoblot shows heart lysates separated into supernatant (s) or pellet (p) after detergent extraction followed by low-speed centrifugation, separation by SDS-PAGE, and transfer to nitrocellulose. PAK immunoreactivity is predominantly cytosolic in control ntg (control) sample, but shifts to the cytoskeletal insoluble fraction in racET samples (racET) from hypertrophic (hyp) and dilated (dil) hearts. Percentage of PAK signal between the supernatant and pellet of each sample (distribution) is shown after correction to GAPDH signals from the same blot (not shown) to control for variances in loading. (**b** and **c**) Confocal microscopy of isolated cardiomyocytes from 21-day-old mice shows cytosolic PAK immunoreactivity (green) in control ntg cell (**b**). In comparison, cardiomyocyte from racET heart (**c**) shows PAK immunoreactivity in a striated pattern (at arrows) with bands between Z-discs (red; labeled with phalloidin). Increased striations of paxillin staining are also evident in the racET cardiomyocyte (blue; labeled with antipaxillin antibody). Relevance of variable nuclear staining observed in cardiomyocytes remains unknown. (**d**–**g**) Redistribution of phosphothreonine immunoreactivity between ntg control (**d** and **e**) or racET (**f** and **g**) cardiomyocytes. Cellular structures of actin filaments (red; labeled with phalloidin) or nuclei (blue; labeled with ToPro dye) were used to identify cardiomyocytes. Phosphothreonine immunoreactivity (green) is distributed in a fibrillar pattern in control cells (**d**), with diffuse striated appearance of antiphosphothreonine label evident at higher magnification (**e**). In comparison, racET cardiomyocytes show diminished fibrillar labeling within the cell interior (**f**) and enhanced reactivity around the cell perimeter shown at higher magnification (**g**). Bar: (**b** and **c**) 10 μm; (**d**–**g**) 20 μm.

hypothyroidism and inhibit thyroid hormone–driven transgene expression. Litters of racET mice were treated with PTU for 2 weeks after birth, and then housed for another week without supplementation prior to sacrifice. This treatment protocol prevented development of the cardiomyopathic changes previously observed in racET mice. Unlike the dilated or hypertrophic changes in untreated racET mice (Figure 2), hearts from PTU-treated racETs were comparable in shape and size (heart/body weight ratio of 7.7 ± 1.9, n = 25) with ntg control hearts maintained on the same PTU treatment protocol (heart/body weight ratio of 7.8 ± 0.6, n = 15). An abbreviated PTU supplementation protocol for 1 week after birth was not sufficient to prevent cardiomyopathic changes in racET mice (data not shown). Together with thyroid hormone manipulation experiments (Figure 1c), these results indicate the racET cardiomyopathic phenotype depends upon postnatal stimulation of rac1 transgene expression by thyroid hormone.

In contrast to the dilated hearts of young racET mice that died spontaneously, hypertrophy became the dominant phenotype in juvenile racET mice by 3 weeks of age. Gross morphology of bisected hearts from racET mice as early as 3 weeks after birth (Figure 2, bottom) showed that overall heart size was not increased. However, heart/body weight ratio (7.5 ± 2.2, n = 77) was significantly elevated (P < 0.0001) compared with ntg controls (5.4 + 0.5, n = 96), which was associated with the thickening of ventricular walls and loss of ventricular chamber area suggestive of concentric hypertrophy. A hypertrophic gene expression profile was evident from total mRNA analysis of hearts of racET mice, demonstrating altered levels including significant elevation of atrial natriuretic factor and β-MHC in combination with decreased α-MHC and skeletal actin (Figure 4). Atria in hypertrophic racET hearts were markedly enlarged by 2 months of age, progressively deteriorating to thin-walled sac-like structures by 6 months of age. It is interesting to note that during this same period of time, the heart/body weight ratios of racET hearts (Figure 3, bottom; 5.9 ± 0.6, n = 20) returned to values comparable to ntg controls (5.5 ± 0.6, n = 34). This normalization of heart/body weight ratio in racET mice occurred despite persistent expression levels of tg rac1 protein by immunoblot analysis from 52 days after birth until 226 of age (Figure 1d). Differential pathogenesis in the deteriorating atria versus improving ventricles suggests these two structures respond differently to activation of the rac1 pathway or that ventricular hemodynamic performance is disturbed despite overtly normal morphology.

Hearts from hypertrophic racET mice are hypercontractile. Hypertrophic racET hearts were hypercontractile relative to the ntg controls (Table 1). Contractility as measured by dP/dt was increased 36% in the working heart subjected to preload and afterload pressure. Contractility was similarly increased by 46% in the nonworking perfused racET heart compared with ntg controls.

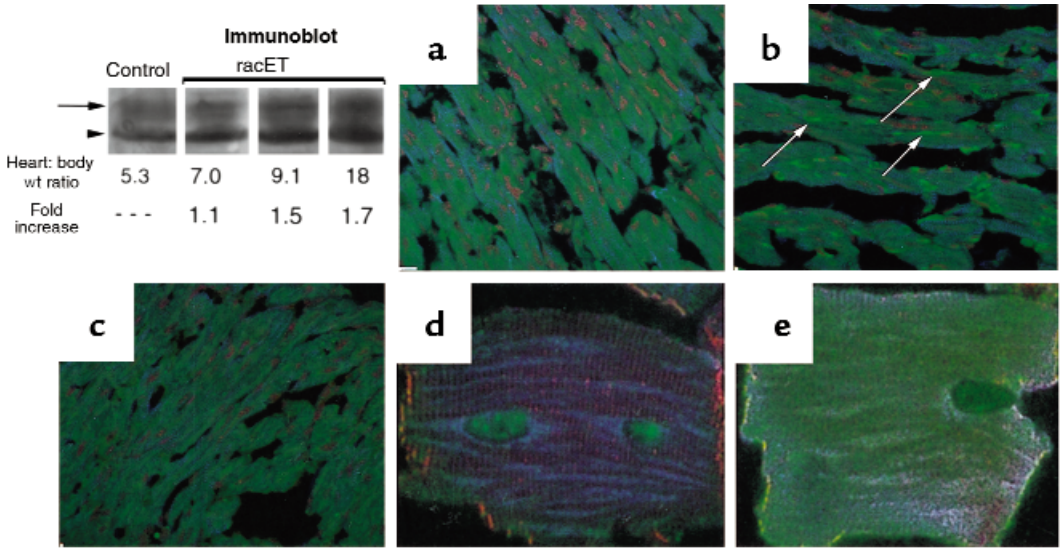

Figure 7
Redistribution of src in racET hearts. Detection of phospho-src by confocal microscopy in heart lysates (Immunoblot), heart sections (**a**–**c**) and isolated cardiomyocytes (**d** and **e**). Immunoblot shows increased phospho-src^{529} labeling in 9- to 11-day-old dilated racET heart samples present as multiple bands, presumably resulting from variation in level of src phosphorylation on multiple residues. Control section (**a**) shows widespread patchy low-level phospho-src^{418} labeling (green, with nuclei in red). In comparison, a section from a dilated heart shows intense focal areas of phospho-src^{418} labeling, often appearing thin and thread-like (**b**, at arrows). Intense staining observed in dilated sample (**b**) is diminished in the hypertrophic racET sample (**c**). Staining is evident within isolated racET cardiomyocytes as phospho-src^{418} reactivity is absent from the cytoplasm of control ntg (**d**), but apparent throughout the cell body and along the periphery of a dilated racET heart cardiomyocyte (**e**). Bar: in **a**–**c** = 20 μm, 5 μm in **d** and **e**.

Impaired relaxation as measured by increased –dP/*dt* in the nonworking racET heart reflects the pathologic condition of these hearts, possibly resulting from thickening of the ventricular wall.

Microscopy shows well-organized myofibrillar structure with subtle cellular abnormalities in racET hearts. Myofibril organization in racET hearts was determined by examining Z-disc integrity, because Z-discs are organizing centers for sarcomeric actin, that often show aberrant structure in cardiomyopathic heart sections (29). Z-discs were visualized by confocal microscopy using antibody to α-actinin, a component protein of the Z-disc. Both ntg control and racET sections show well-organized repeating striations of α-actinin labeling, indicative of mature myofibrils (Figure 5, top), with no evidence of overt myofibril disarray. However, subtle Z-disc abnormalities not apparent by light microscopy can be revealed by electron microscopy (30). Ultrastructural analysis showed both ntg and dilated racET heart sections had well-organized myofibrils with clearly defined bands in both I-Z-I and A regions (data not shown). Comparison of cellular structure revealed decreased myofibril density in the central area of some dilated racET cardiomyocytes filled with granular material (Figure 5e, at "g"). The relationship of the granular material to the observed phenotype of dilation is unknown, but similar observations have been made in cultured cardiomyocytes after mechanically induced stretch (unpublished observations).

Signal transduction cascades regulating focal adhesion are altered in racET hearts. A primary downstream target of rac1 signaling is PAK (17), a serine/threonine kinase associated with disassembly of stress fibers and loss of focal adhesion complexes (31, 32). Evidence for activation of PAK was found by using both immunoblot and confocal microscopy. Heart lysates from ntg controls and racET mice were separated by centrifugation into cytosol and cytoskeletal fractions based on solubility in 0.1% Triton X-100 detergent. PAK reactivity was present in both fractions in all samples, but PAK distribution shifted from primarily cytosol in ntg controls to cytoskeletal in racET samples (Figure 6a). PAK distribution in racET samples showed a trend toward increasing solubility in older animals (Figure 6a, compare racET hyp at day 15 with day 21). Subtle PAK distribution changes were difficult to resolve in tissue sections (data not shown), but differences became apparent upon examination of isolated cardiomyocytes from control ntg and racET hearts (Figure 6 b and c). Control cardiomyocytes labeled for PAK showed diffuse low-level reactivity as wispy broad bands running parallel to the length of myofibrils throughout the cell interior (Figure 6b). In comparison, anti-PAK immunoreactivity was increased in racET cells with labeling present as faint parallel striations between Z-discs as well as enhanced perinuclear staining (Figure 6c, arrows). Because PAK phosphorylates serine/threonine residues, isolated cardiomyocytes were labeled with antiphosphothreonine anti-

body to check for altered phosphorylation patterns (Figure 6, d–g). Phosphothreonine reactivity patterns in control ntg cardiomyocytes consisted of extensive fibrillar labeling throughout the cell in parallel with myofibrils (Figure 6, d and e). A different pattern was evident in racET cardiomyocytes as the fibrillar interior labeling was lost, but intense punctate reactivity appeared along the cell periphery (Figure 6, f and g). Phosphoserine reactivity patterns were similar to those described for phosphothreonine, although staining was less intense (not shown).

Activation of PAK and phosphothreonine redistribution (Figure 6), together with reports of PAK influence upon cell morphology and adhesion (31, 32), suggested phosphorylation of regulatory proteins associated with focal adhesion complexes may be affected in racET hearts. Two primary regulators of focal adhesion structure are the kinases FAK and src, which participate in cardiac responses to growth or disease (33, 34). Levels and distribution of serine- or tyrosine-phosphorylated FAK were comparable between control ntg and racET heart samples (data not shown). However, immunoblot experiments showed increased accumulation of phospho-src^{529} in dilated racET heart samples compared with an age matched ntg control (Figure 7, Immunoblot). A threadlike and patchy pattern of altered phospho-src^{418} distribution was observed in dilated racET heart sections (Figure 7b, at arrows). Increased phospho-src^{418} immunoreactivity was observed in cardiomyocytes isolated from dilated racET hearts (Figure 7e) compared with ntg controls (Figure 7d). These results suggest that altered src signaling may be important in the pathogenesis of racET dilation.

Src signaling acts on paxillin, a phosphorylation substrate located at focal adhesion complexes (35). Lysates were prepared and immunoprecipitation was performed with antipaxillin antibody to enrich for paxillin protein. Phospho-paxillin^{31} was present in both ntg controls as well as racET hearts at comparable levels, as shown by immunoblot; dilated racET samples consistently showed slight, albeit statistically insignificant (10%), increases in immunoreactivity (Figure 8). Reactivity in control samples indicated that phospho-paxillin^{31} is normally present within cells of the myocardium at this age, although the distinction between expression in cardiomyocytes versus nonmyocytes cannot be made by immunoblot analysis. Heart sections of controls labeled with antibody to phospho-paxillin^{31} showed widespread patchy labeling throughout the section (Figure 8, control). In comparison, sections from both dilated and hypertrophic racET hearts showed marked striations of phospho-paxillin^{31} label (Figure 8, dilated and hypertrophic).

Expression of V12rac1 protein induces changes in cultured cardiomyocytes similar to racET hearts. Effects of rac1 signaling on PAK and paxillin, the presumptive downstream target proteins of rac1 activation in vivo (Figures 6 and 8), were examined in vitro to demonstrate consequences of rac1 activity in cultured cardiomyocytes. Cultures were infected with adenovirus expressing constitutively activated rac1 protein or β-galactosidase as a control. PAK association with the cytoskeletal fraction was increased by 65% in cultures after rac1 expression as measured by immunoblot analysis (Figure 9, top; average was 20% in controls versus 33% with rac1). PAK and phosphothreonine immunoreactivity of cultured cells was also enhanced after rac1 infection as observed by confocal microscopy (not shown). Confocal microscopy demonstrated altered phos-

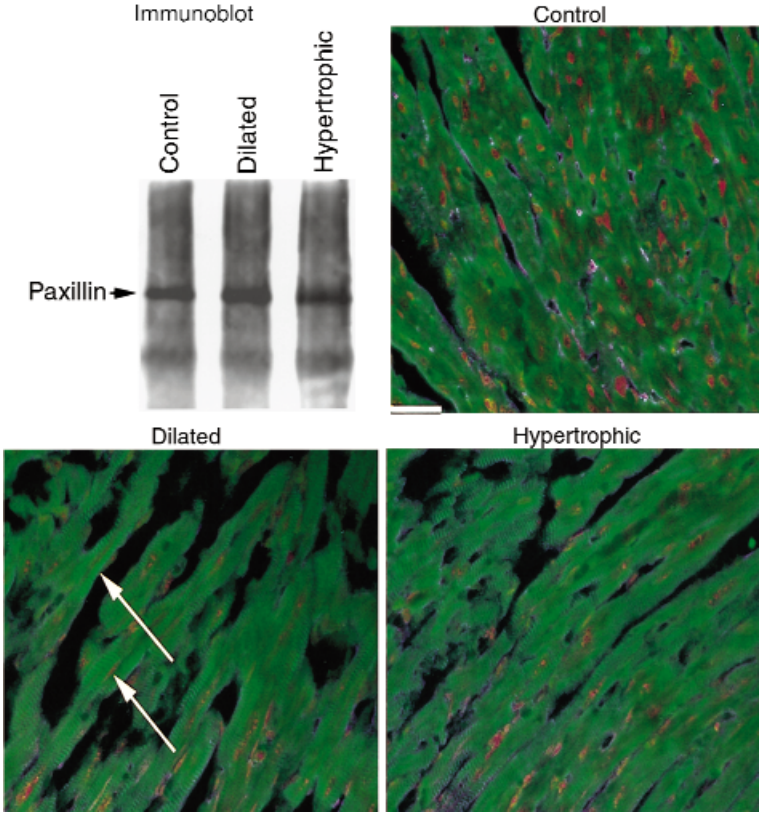

Figure 8
Changes in paxillin phosphorylation correlate with racET cardiomyopathy. Detection of phosphorylation of paxillin at tyrosine residue 31 with antiphospho-paxillin^{31} antibody by immunoblot and confocal microscopy. For immunoblot, paxillin was enriched from heart lysates by immunoprecipitation, separated from associated proteins by SDS-PAGE, blotted, and labeled with antiphospho-paxillin antibody. Detected paxillin at 68 kDa is indicated (arrow), which shows insignificant differences in level between the 3 samples. Confocal microscopy shows widespread patchy labeling in control ntg section. In comparison, racET sections show marked striations of immunoreactivity (at arrows) indicative of altered phospho-paxillin^{31} distribution in cardiomyocytes. Bar = 20 μm.

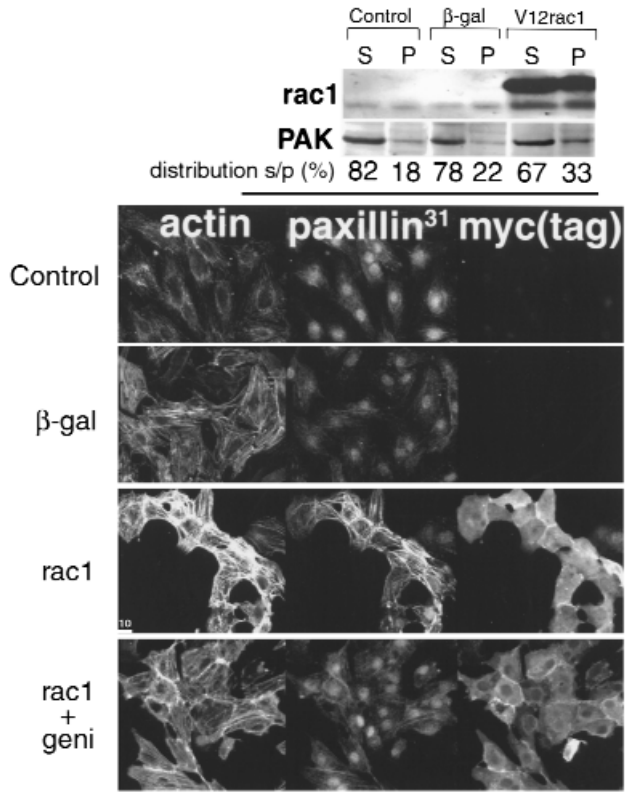

Figure 9
Changes observed in racET hearts can be recapitulated in cultured cardiomyocytes after expression of constitutively activated rac1 protein. Neonatal rat cardiomyocytes were infected with adenoviruses producing β-gal or constitutively activated myc-tagged rac1 protein. Consequences of rac1 pathway activation upon PAK association with the cytoskeletal fraction were assessed by immunoblot (top) and distribution of phospho-paxillin[31] was observed by confocal microscopy (bottom). The immunoblot shows approximately 20% of PAK is associated with the cytoskeletal fraction in uninfected or β-gal–infected cultures, with an increase of up to 33% after rac1 infection. Microscopy demonstrates myofibril organization labeled by phalloidin (actin), phospho-paxillin[31] immunoreactivity (paxillin[31]), and infection revealed by myc [myc(tag)]. Myofibril organization appears enhanced by rac1 expression (rac1, actin) as well as phospho-paxillin[31] labeling coincident with myofibril striations (rac1, paxillin[31]). Inhibition of tyrosine kinase activity by addition of genistein mitigates increased myofibril organization and phospho-paxillin[31] immunoreactivity (rac1 + geni). Nuclear reactivity, which was never observed in vivo, is presumed to be related to culture conditions. Bar: 10.0 μm.

pho-paxillin[31] immunoreactivity after rac1 infection, with phospho-paxillin[31] localization coincident with striations of myofibrils (Figure 9, paxillin[31]). The hypertrophic effect of rac1 activation caused enhanced sarcomeric organization, as revealed by phalloidin labeling (Figure 9, actin). Infection was confirmed by myc tag staining of the transgene (Figure 9, myc(tag)). Enhancement of phospho-paxillin[31] labeling was inhibited by addition of a tyrosine kinase inhibitor, genistein, after infection (Figure 9, rac1+geni). Genistein also decreased — but did not eliminate — the effect of rac1 on myofibril organization, as shown by diminished actin filament labeling. These results indicate that activation of rac1 affects the same target proteins in vivo and in vitro, as well as demonstrating that tyrosine kinase activation plays an important role in rac1-mediated effects.

Discussion

Activation of rac1 signaling produced dramatic cardiomyopathic phenotypes in young racET mice (Figure 2). Low level of transgene expression, consistent with endogenous protein level (Figure 1), supports the conclusion that rac1-specific signaling activation causes cardiomyopathy rather than secondary consequences of high level transgene expression (36). Lethal dilation occurred exclusively in young mice (Figure 3, top), and elevation of postnatal rac1 expression by T^3 supplementation increased both frequency and severity of the dilated cardiomyopathy (Figures 1c, and 2, middle). Association between postnatal development, rac1 activation, and lethal dilated cardiomyopathy, suggests heightened sensitivity of the neonatal heart to rac1-mediated effects. However, circumstantial evidence suggests myocardial desensitization to activated rac signaling 2–4 weeks after birth, demonstrated by normalization of heart/body weight ratio (Figure 3) and shifting PAK distribution from cytoskeletal to cytosolic fractions (Figure 6).

PAK-mediated cytoskeletal remodeling (31) could be influenced by recruitment of PAK to focal adhesions in a multimolecular complex targeted to paxillin (37). Paxillin possesses multiple binding domains for regulatory kinases that regulate assembly of focal adhesions (38). Phosphorylation of paxillin by regulatory tyrosine kinases such as FAK and src has been well documented (35, 39), and recent reports indicate that serine/threonine phosphorylation of paxillin can influence organization of focal adhesions and cellular adhesion (40). Absence of overt myofibril disruption in racET cardiomyocytes (Figure 6) suggests that heart failure in young racET mice is not caused by loss of myofibril organization as previously described for tropomodulin-overexpressing tg mice (23). Instead, we favor the hypothesis that deregulation of signaling by rac1 and PAK, followed by loss of cellular adhesion, leads to impaired force transmission, loss of systolic function, and lethal dilated cardiomyopathy in young racET mice.

In contrast to the dramatic phenotype of racET dilation, the impact of rac1 expression appeared to diminish as mice age, as evidenced by analysis of hearts from older racET mice (Figures 2, bottom, and 3, bottom). Regression of heart/body weight ratio in older racET mice was not caused by loss of transgene expression, which persisted beyond the first 6 months of life (Figure 1d). Perhaps decreased downstream PAK-mediated signaling slows progression of ongoing hypertrophy that has developed by 3 weeks after birth. At present, studies regarding PAK activation in cultured cardiomyocytes have been limited in scope (41), and this study is the first experimental examination of cardiac PAK activation in vivo. Ongoing studies with racET

mice will undoubtedly provide additional insight into the role of PAK activation in cardiac remodeling and focal adhesion reorganization.

The molecular signaling connection between rac1 and the actin cytoskeleton is an area of intense ongoing research with recent interest focusing on the participation of PAK. Effects of rac1 on cytoskeletal organization are mediated, in part, by activation of PAK (42, 43), which phosphorylates serine/threonine residues. Activation of PAK, like rac1, leads to disassembly of focal adhesion complexes (31). In addition, PAK can also counteract the activity of RhoA (a hypertrophic stimulus) resulting in disassembly of stress fibers (44).

Additional undiscovered molecular connections exist between rac, PAK, and the actin cytoskeleton, because evidence exists for both rac1 regulation of the cytoskeleton independent of PAK action (16) and PAK action on the cytoskeleton upstream of rac1 (45). PAK remains a prime candidate to exert effects upon cell adhesion because of its colocalization at focal adhesions with PAK-interacting exchange factor (PIX), a rac guanine exchange factor that participates in regulation of PAK-mediated rac activation (45, 46). PAK's interaction with paxillin is mediated via a recently discovered paxillin-kinase linker that binds directly to paxillin and PIX (36). Additional studies are needed to investigate the rac1/PAK axis in cardiac remodeling and to assess the participation of cofactors such as PIX and paxillin-kinase linker in PAK targeting.

Signaling pathways involving phosphorylation are taking an increasingly prominent role in explaining the molecular pathogenesis of cardiomyopathy (47). Undoubtedly, regulation of kinase activity is critical for normal cardiac structure and function. Disturbing the normal balance of protein phosphorylation results in cardiac hypertrophy, as shown by activation of protein kinase C (48) or calcineurin phosphatase (49). Cross-talk between molecular pathways in the myocardium — also known as multiplex signaling — plays a pivotal role in the determination of the phenotypic response (50). Multiplex signaling may be involved in the determination of racET phenotype as well, because phospho-src^{418} redistribution correlates with dilation in young racET mice (Figure 8). Although there are multiple possibilities for signaling in racET mice, a tempting, albeit reductionist, starting hypothesis is to speculate that the combination of src and rac1/PAK activation is responsible for the pathogenesis of racET dilation. Activated src participates in tyrosine phosphorylation of paxillin (35), and striations of tyrosine-phosphorylated paxillin became apparent in young racET hearts, consistent with the ongoing reorganization of focal adhesions likely to occur in a remodeling myocardium. This intriguing novel observation implicates paxillin phosphorylation in the pathogenesis of cardiomyopathy and presents the possibility of multiple phosphorylations occurring on tyrosine as well as serine/threonine sites throughout the molecule. The tyrosine 31 residue of paxillin appears phosphorylated in racET hearts regardless of phenotype, so it will be interesting to characterize the relevance of this observation to other myocardial conditions where remodeling occurs.

Unraveling the details of ras family–mediated signaling in the myocardium is complicated by at least 2 phenomena. First, ras family members can affect multiple signaling pathways upon activation, and second, signaling crossover occurs between ras family proteins and their downstream targets. This complexity probably accounts for the variety of phenotypic consequences observed after alteration of ras family signaling. The association of ras with hypertrophy (9, 10), the paradoxical correlation of rhoA with hypertrophy in vitro but not in vivo (6, 11, 13), and rac1 promoting dilation (this study) and hypertrophy (5) collectively define the challenge remaining: to define relationships between ras family activation and cardiac remodeling.

The answers are likely to be found by studying the consequences of shifting timing, intensity, and activation of concurrent multiple signaling pathways. The critical nature of timing and intensity is apparent because, depending upon postnatal expression level, rac1-mediated signaling initiated two completely different cardiomyopathic responses (dilation or hypertrophy). Both cardiomyopathic phenotypes affect signaling pathways regulating cellular adhesion via PAK activation, but concurrent changes in src-mediated signaling may contribute to cytoskeletal remodeling.

Acknowledgments

This research was funded by grants from the National Institutes of Health (HL58224-02) and the American Heart Association National Organization (9750638N) (both to M. A. Sussman). Thanks to Jon Neuman for creation of our original racET mice. We are grateful to Jeffrey Molkentin and Jeffrey Robbins for helpful discussions, and to Leon DeWindt, Hae Lim, and Kevin Tymitz for preparations of cultured cardiomyocytes.

1. Van Aelst, L., and D'Souza-Schorey, C. 1997. Rho GTPases and signaling networks. *Genes Dev.* **11**:2295–2322.
2. Tapon, N., and Hall, A. 1997. Rho, Rac and Cdc42 GTPases regulate the organization of the actin cytoskeleton. *Curr. Opin. Cell Biol.* **9**:86–92.
3. Ridley, A.J. 1996. Rho: theme and variations. *Curr. Biol.* **6**:1256–1264.
4. Ridley, A.J., Paterson, H.F., Johnston, C.L., Diekmann, D., and Hall, A. 1992. The small GTP-binding protein rac regulates growth factor-induced membrane ruffling. *Cell.* **70**:401–410.
5. Pracyk, J.B., et al. 1998. A requirement for the rac1 GTPase in the signal transduction pathway leading to cardiac myocyte hypertrophy. *J. Clin. Invest.* **102**:929–937.
6. Hoshijima, M., Sah, V.P., Wang, Y., Chien, K.R., and Brown, J.H. 1998. The low molecular weight GTPase Rho regulates myofibril formation and organization in neonatal rat ventricular cardiomyocytes. Involvement of rho kinase. *J. Biol. Chem.* **273**:7725–7730.
7. Wang, S.-M., Tsai, Y.-J., Jiang, M.-J., and Tseng, Y.-Z. 1997. Studies on the function of rhoA protein in cardiac myofibrillogenesis. *J. Cell. Biochem.* **66**:43–53.
8. Thorburn, J., Xu, S., and Thorburn, A. 1997. MAP kinase and rho-dependent signals interact to regulate gene expression but not actin morphology in cardiac muscle cells. *EMBO J.* **16**:1888–1900.
9. Fuller, S.J., Gillespie-Brown, J., and Sugden, P. 1998. Oncogenic src, raf, and ras stimulate a hypertrophic pattern of gene expression and increase cell size in neonatal rat ventricular myocytes. *J. Biol. Chem.* **273**:18146–18152.
10. Hunter, J.J., Tanaka, N., Rockman, H.A., Ross, J., Jr., and Chien, K.R. 1995. Ventricular expression of a MLC-2v-ras fusion gene induces cardiac hypertrophy and selective diastolic dysfunction in transgenic mice. *J. Biol. Chem.* **270**:23173–23178.
11. Sah, V.P., et al. 1999. Cardiac-specific overexpression of RhoA results in

sinus and atrioventricular nodal dysfunction and contractile failure. *J. Clin. Invest.* **103**:1627–1634.
12. Sah, V.P., Hoshijima, M., Chien, K.R., and Brown, J.H. 1996. Rho is required for $G\alpha_q$ and α_1-adrenergic receptor signaling in cardiomyocytes. *J. Biol. Chem.* **271**:31185–31190.
13. Hines, W.A., and Thorburn, A. 1998. Ras and rho are required for $G\alpha_q$–induced hypertrophic gene expression in neonatal rat cardiac myocytes. *J. Mol. Cell. Cardiol.* **30**:485–484.
14. Zechner, D., Thuerauf, D.J., Hanford, D.S., McDonough, P.M., and Glembotski, C.C. 1997. A role for the p38 mitogen-activated protein kinase pathway in myocardial cell growth, sarcomeric organization, and cardiac-specific gene expression. *J. Cell Biol.* **139**:115–127.
15. Aikawa, R., et al. 1999. Rho family small G proteins play critical roles in mechanical stress-induced hypertrophic responses in cardiac myocytes. *Circ. Res.* **84**:458–466.
16. Westwick, J.K., et al. 1997. Rac regulation of transformation, gene expression, and actin organization by multiple, PAK-independent pathways. *Mol. Cell Biol.* 1324–1335.
17. Manser, E., Leung, T., Salihuddin, H., Zhao Z.-S., and Lim, L. 1994. A brain serine/threonine protein kinase activated by cdc42 and rac1. *Nature.* **367**:40–46.
18. Flinn, H.M., and Ridley, A.J. 1996. Rho stimulates tyrosine phosphorylation of focal adhesion kinase, p130 and paxillin. *J. Cell Sci.* **109**:1133–1141.
19. Wang, Y., et al. 1998. Cardiac hypertrophy induced by mitogen-activated protein kinase kinase 7, a specific activator for c-Jun NH_2-terminal kinase in ventricular muscle cells. *J. Biol. Chem.* **273**:5423–5426.
20. Gulick, J., Subramaniam, A., Neumann, J., and Robbins, J. 1991. Isolation and characterization of the mouse cardiac myosin heavy chain genes. *J. Biol. Chem.* **266**:9180–9185.
21. Rindt, H., Subramaniam, A., and Robbins, J. 1995. An in vivo analysis of transcriptional elements in the mouse α-myosin heavy chain gene promoter. *Transgenic. Res.* **4**:397–405.
22. Diekmann, D., et al. 1991. *Bcr* encodes a GTPase-activating protein for $p21^{rac}$. *Nature.* **351**:400–402.
23. Sussman, M.A., et al. 1998. Myofibril degeneration caused by tropomodulin overexpression leads to dilated cardiomyopathy in juvenile mice. *J. Clin. Invest.* **101**:51–61.
24. Gemmill, C.L. 1956. Metabolic effects of thyroxine, 3,3',5-triiodothyronine, 3,3′-diiodo-5-bromothyronine and 3,3′-diiodothyronine administered orally to rats. *Am. J. Physiol.* **187**:323–327.
25. Tsika, R.W., Bahl, J.J., Leinwand, L.A., and Morkin, E. 1990. Thyroid hormone regulates expression of a transfected human α-myosin heavy chain fusion gene in fetal rat heart cells. *Proc. Natl. Acad. Sci. USA.* **87**:379–383.
26. Cambon, N., and Sussman, M.A. 1997. Isolation and preparation of single mouse cardiomyocytes for fluorescence confocal microscopy. *Methods Cell Sci.* **19**:83–90.
27. Perks, C.M., Newcomb, P.V., Norman, M.R., and Holly, J.M.P. 1999. Effect of insulin-like growth factor binding protein-1 on integrin signalling and the induction of apoptosis in human breast cancer cells. *J. Mol. Endocrin.* **22**:141–150.
28. Sussman, M.A., et al. 1998. Altered expression of tropomodulin in cardiomyocytes disrupts the sarcomeric structure of myofibrils. *Circ. Res.* **82**:94–105.
29. Schaper, J., et al. 1991. Impairment of the myocardial ultrastructure and changes of the cytoskeleton in dilated cardiomyopathy. *Circulation.* **83**:504–514.
30. Sussman, M.A., et al. 1999. Pathogenesis of dilated cardiomyopathy: molecular, structural, and population analyses in tropomodulin overexpressing transgenics. *Am. J. Pathol.* **155**:2101–2113.
31. Manser, E., et al. 1997. Expression of constitutively active α-PAK reveals effects of the kinase on actin and focal complexes. *Mol. Cell. Biol.* **17**:1129–1143.
32. Sells, M.A., Boyd, J.T., and Chernoff, J. 1999. p21-activated kinase (Pak1) regulates cell motility in mammalian fibroblasts. *J. Cell. Biol.* **145**:837–849.
33. Kuppuswamy, D., et al. 1997. Association of tyrosine-phosphorylated c-src with the cytoskeleton of hypertrophying myocardium. *J. Biol. Chem.* **272**:4500–4508.
34. Kovacic, B., Ilic, D., Damsky, C.H., and Gardner, D.G. 1998. C-Src activation plays a role in endothelin-dependent hypertrophy of the cardiac myocyte. *J. Biol. Chem.* **273**:35185–35193.
35. Brown, M.T., and Cooper, J.A. 1996. Regulation, substrates and functions of src. *Biochim. Biophys. Acta.* **1287**:121–149.
36. James, J., et al. 1999. Transgenic over-expression of a motor protein at high levels results in severe cardiac pathology. *Transgenic Res.* **8**:9–22.
37. Turner, C.E., et al. 1999. Paxillin LD4 Motif binds PAK and PIX through a novel 95-kD ankyrin repeat, ARF-GAP protein: a role in cytoskeletal remodeling. *J. Cell Biol.* **145**:851–863.
38. Turner, C.E. 1998. Paxillin. *Int. J. Biochem. Cell Biol.* **30**:955–959.
39. Bellis, S.L., Miller, J.T., and Turner, C.E. 1995. Characterization of tyrosine phosphorylation of paxillin *in vitro* by focal adhesion kinase. *J. Biol. Chem.* **270**:17437–17441.
40. Brown, M.C., Perrotta, J.A., and Turner, C.E. 1998. Serine and threonine phosphorylation of the paxillin LIM domains regulates paxillin focal adhesion localization and cell adhesion to fibronectin. *Mol. Biol. Cell.* **9**:1803–1816.
41. Clerk, A., and Sugden, P.H. 1997. Activation of p21-activated protein kinase alpha (alpha PAK) by hyperosmotic shock in neonatal ventricular cardiomyocytes. *FEBS Lett.* **403**:23–25.
42. Frost, J.A., Khokhlatchev, A., Stippec, S., White, M.A., and Cobb, M.H. 1998. Differential effects of PAK1-activating mutations reveal activity-dependent and -independent effects on cytoskeketal regulation. *J. Biol. Chem.* **273**:28191–28198.
43. Eby, J.J., et al. 1998. Actin cytoskeleton organization regulated by the PAK family of protein kinases. *Curr. Biol.* **8**:967–970.
44. Sanders, L.C., Matsumura, F., Bokoch, G.M., and de Lanerolle, P. 1999. Inhibition of myosin light chain kinase by p21-activated kinase. *Science.* **283**:2083–2085.
45. Obermeier, A., et al. 1998. PAK promotes morphological changes by acting upstream of rac. *EMBO J.* **17**:4328–4339.
46. Daniels, R.H., Zenke, F.T., and Bokoch, G.M. 1999. A pix stimulates p21-activated kinase activity through exchange factor-dependent and -independent mechanisms. *J. Biol. Chem.* **274**:6947–6050.
47. Yamazaki, T., Komuro, I., and Yazaki, Y. 1998. Signalling pathways for cardiac hypertrophy. *Cell. Signal.* **10**:693–698.
48. Bowman, J.C., et al. 1997. Expression of protein kinase C β in the heart causes hypertrophy in adult mice and sudden death in neonates. *J. Clin. Invest.* **100**:2189–2195.
49. Sussman, M.A., et al. 1998. Prevention of cardiac hypertrophy in mice by calcineurin inhibition. *Science.* **281**:1690–1693.
50. Denhardt, D.T. 1996. Signal-transducing protein phosphorylation cascades mediated by Ras/Rho proteins in the mammalian cell: the potential for multiplex signalling. *Biochem. J.* **318**:729–747.
51. Price, R.L., Chintanowonges, C., Shiraishi, I., Borg, T.K., and Terracio, L. 1996. Local and regional variations in myofibrillar patterns in looping rat hearts. *Anat. Rec.* **245**:83–93.
52. Gulick, J., et al. 1997. Transgenic remodeling of the regulatory myosin light chains in the mammalian heart. *Circ. Res.* **80**:665–664.